

FIG. 2. Components of the atom-to-metal shifts. $\delta E_B^*(nl)$ is the effective ("metal-atom"-to-metal) shift which corresponds to both atomic and metallic configurations having the $4f$ occupancy of the solid. $\Delta E_B^{\text{config}}(nl)$ represents the modification of the free-atom nl binding energy arising from the change to the metallike configuration.

absence of such a change. Figure 2 displays these two components.

It is apparent from Fig. 2 that $\delta E_B^*(nl)$ is essentially independent of nl . The shifts are regularized when no configuration change occurs, showing only a slight decrease across the series which is associated with the lanthanide contraction (an effect also noted in Ref. 6). Comparison of Figs. 1 and 2 makes it evident that $\Delta E_B^{\text{config}}$ is responsible both for the distinction between the δE_B results for Pr-Sm, Tb-Tm and the other elements, as well as for the differences among the shifts

for each member of the former group. The shifts for Pr-Sm and Tb-Tm are reduced because $\Delta E_B^{\text{config}} < 0$ for those elements. This is a consequence of the fact that $E_B^* > E_B^{\text{atom}}$ when the metallike configuration has one fewer $4f$ electron and, hence, greater effective nuclear charge, than the ground atomic configuration.

It is a pleasure to acknowledge productive discussions with J. W. Wilkins and J. R. Smith.

¹L. Ley, S. P. Kowalczyk, F. R. McFeely, R. A. Pollak, and D. A. Shirley, Phys. Rev. B **8**, 2392 (1973).

²R. E. Watson and M. L. Perlman, Struct. Bonding **24**, 83 (1975).

³R. W. Watson, M. L. Perlman, and J. F. Herbst, Phys. Rev. B **13**, 2358 (1976).

⁴D. A. Shirley, R. L. Martin, S. P. Kowalczyk, F. R. McFeely, and L. Ley, Phys. Rev. B **15**, 54 (1977).

⁵A. R. Williams and N. D. Lang, Phys. Rev. Lett. **40**, 954 (1978).

⁶B. Johansson and N. Mårtensson, Phys. Rev. B **21**, 4427 (1980).

⁷J. F. Herbst and J. W. Wilkins, Phys. Rev. B **26**, 1689 (1982) ($2p$ levels).

⁸J. F. Herbst and J. W. Wilkins, Phys. Rev. B **20**, 2999 (1979) ($3d$ levels).

⁹J. F. Herbst, R. E. Watson, and J. W. Wilkins, Phys. Rev. B **13**, 1439 (1976) (occupied $4f$ levels).

¹⁰J. F. Herbst, R. E. Watson, and Y. Baer, Phys. Rev. B **16**, 2447 (1977) ($5s$ levels).

¹¹A. Rosengren and B. Johansson, Phys. Rev. B **22**, 3706 (1980).

Bound State between a Crystal-Field Excitation and a Phonon in CeAl_2

Peter Thalmeier and Peter Fulde

Max-Planck-Institut für Festkörperforschung, D-7000 Stuttgart 80, Federal Republic of Germany

(Received 10 September 1982)

The existence of a bound state between a crystal-field excitation and a low-lying phonon in CeAl_2 is suggested. It can explain in a natural way the hitherto unexplained two-peak structure found in magnetic neutron-scattering experiments. Various checks are made to substantiate this suggestion. A similarity is pointed out to the exciton-phonon bound-state problem in semiconductors.

PACS numbers: 75.10.Dg, 63.20.Kr, 71.70.Ch

The intermetallic cubic Laves-phase material CeAl_2 , in which the Ce ions have a stable 3^+ configuration with $J = \frac{5}{2}$, has attracted considerable attention for various reasons. At low temperatures the system exhibits a Kondo effect ($T_K \approx 6$ K) and antiferromagnetic order ($T_N = 3.9$ K).^{1,2} It

also shows a strong magnetoelastic coupling leading to pronounced low-temperature anomalies in the c_{44} elastic constant.³ One striking observation⁴ is the appearance of two inelastic lines in inelastic magnetic neutron-scattering experiments at energies $\Delta_1 = 100$ K and $\Delta_2 = 180$ K. This

is contrary to expectations since the cubic crystal-line electric field (CEF) at a Ce site should split the $J = \frac{5}{2}$ ground state into a Γ_7 doublet and a Γ_8 quartet resulting in *one* inelastic line only. Indeed, the analysis of thermodynamic, transport, and magnetoelastic properties usually assumes a CEF scheme like the one shown in Fig. 1(a) with $\Delta = 100$ K. There is strong evidence that the observed two inelastic transitions must originate from the $\Gamma_7 \rightarrow \Gamma_8$ inelastic excitation. The sum of the integrated intensities of the two peaks $I_{in} = I_{in}^{(1)} + I_{in}^{(2)}$ relates to the integrated quasi-elastic scattering I_{el} as $I_{in}/I_{el} = 3.2$.⁴ This coincides with the expected ratio of the $\Gamma_7 \rightarrow \Gamma_8$ and $\Gamma_7 \leftrightarrow \Gamma_7$ transitions. Attempts to explain the two-peak structure by a dynamical Jahn-Teller effect (DJTE) in the Γ_8 multiplet were unsuccessful.⁴

It is the aim of this Letter to present strong evidence that the observed two-peak structure is due to a bound state between a CEF excitation and a low-lying phonon. Our starting point is the experimental observation⁵ that the phonon density of states measured at room temperature shows a strong peak around $\hbar\omega_0 = 140$ K. To this peak there contribute three acoustic and three optical phonon branches.⁵ They correspond to vibrations within the diamond-type Ce^{3+} lattice alone. The same peak in the density of states has been observed in $LaAl_2$.⁵ Phonons that include relative motions of the Al ions have corresponding energies > 230 K and are neglected here. The energy $\hbar\omega_0$ is therefore just between the two excitation energies Δ_1 and Δ_2 [Fig. 1(b)].

It is known that inelastic magnetic and phonon scattering compete with each other. But the two contributions can be separated in the standard way because of their different behavior as function of momentum transfer.

We decompose the lattice vibrations which contribute to the peak in the density of states according to representations Γ of the rare-earth ions'

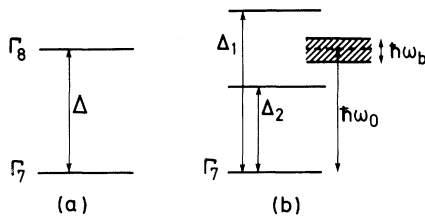


FIG. 1. Schematic representation of (a) the expected and (b) the observed CEF levels in $CeAl_2$. The shaded region in (b) corresponds to energies with high phonon density of states.

cubic point group. The largest contribution to the density-of-states peak comes from the region around the X point where the dispersion curves are very flat and the LO-TO as well as the LA-TA splittings are found to be very small.⁵ Group-theoretical arguments show that the local distortions are mainly of Γ_5 character.

Our model assumption will be that only the Γ_5 part couples to the CEF levels of the Ce^{3+} ions. This is suggested by ultrasonic measurements³ and point-charge calculations⁷ which show that the other coupling constants are much smaller.

For a description of the coupled system of CEF levels and phonons we set $H = H_0 + H_{int}$ where the noninteracting part of the Hamiltonian is given by

$$H_0 = \sum_{\alpha n} \epsilon_{\alpha} |\Gamma_{\alpha}^n\rangle \langle \Gamma_{\alpha}^n| + \hbar\omega_0 \sum_{\mu} (a_{\mu}^{\dagger} a_{\mu} + \frac{1}{2}). \quad (1)$$

The first term describes the CEF levels of Ce^{3+} at a given site. The $|\Gamma_{\alpha}^n\rangle$ are the CEF states characterized by the type of multiplet α and the degeneracy index n . For their explicit form see Ref. 6. The ϵ_{α} denote the CEF energies $\epsilon_7 = 0$ (Γ_7) and $\epsilon_8 = \Delta$ (Γ_8). This Δ is unknown and we shall simply take the mean value $\Delta = \frac{1}{2}(\Delta_1 + \Delta_2) = 140$ K for it. Our final results are not sensitive to the fact that Δ and $\hbar\omega_0$ coincide within the present choice. The second term in Eq. (1) describes the phonons with μ denoting the three polarizations of the Γ_5 vibrations. For simplicity we neglect any phonon dispersion.

The three degenerate vibrational modes couple to the Γ_7 and Γ_8 states by distorting the cubic CEF at the tetragonal Ce sites. This is described by

$$H_{int} = -g_0 \sum_{\mu} (a_{\mu} + a_{\mu}^{\dagger}) O_{\mu}. \quad (2)$$

The quadrupolar operators of Γ_5 symmetry are given by $O_1 = J_y J_z + J_z J_y$, $O_2 = J_z J_x + J_x J_z$, and $O_3 = J_x J_y + J_y J_x$. Computations of the oscillator strengths $Q_{\alpha\beta} = \sum_{nm} |\langle \Gamma_{\alpha}^m | O_{\mu} | \Gamma_{\beta}^n \rangle|^2$ reveal that the Γ_7 - Γ_8 transition couples ten times more strongly to the lattice than do the Γ_8 - Γ_8 transitions.

In constructing the eigenstates of H account is taken of the fact that the product eigenstates to H_0 $|\Gamma_7^n, \mu\rangle = a_{\mu}^{\dagger} |\Gamma_7^n, 0\rangle$ and $|\Gamma_8^n, 0\rangle$ are nearly degenerate. Therefore we choose the following twelve-dimensional subspace $|\varphi_{\kappa}\rangle$ ($\kappa = 1, \dots, 12$) for diagonalization of H : $|\Gamma_7^n, 0\rangle$, $|\Gamma_8^n, 0\rangle$, and $|\Gamma_7^n, \mu\rangle$. The $|\Gamma_8^n, \mu\rangle$ have an energy of $\Delta + \hbar\omega_0 \approx 280$ K and are neglected. The vibronic energies and states are obtained by diagonalizing the matrix $H_{\kappa'\kappa} = \langle \varphi_{\kappa'} | H | \varphi_{\kappa} \rangle$. Their symmetry proper-

ties can be obtained by observing that $|\Gamma_7, \mu\rangle \simeq \Gamma_7 \otimes \Gamma_5 = \Gamma_6 \oplus \Gamma_8$. Therefore the vibronic eigenstates of H^v consist of two doublets $\tilde{\Gamma}_6, \tilde{\Gamma}_7$ and two quartets $\tilde{\Gamma}_{81}, \tilde{\Gamma}_{82}$. Together with their energies they are given by

$$\begin{aligned} |\tilde{\Gamma}_7^n\rangle &= |\Gamma_7^n, 0\rangle, \quad E_7 = 0, \\ |\tilde{\Gamma}_6^n\rangle &= \sum_{m\mu} c_{nm\mu} |\Gamma_7^m, \mu\rangle, \quad E_6 = \hbar\omega_0, \\ |\tilde{\Gamma}_{8i}^n\rangle &= \sum_m a_{nm}^i |\Gamma_8^m, 0\rangle + \sum_{m\mu} b_{nm\mu}^i |\Gamma_7^m, \mu\rangle, \\ E_{8i} &= \frac{1}{2}(\Delta + \hbar\omega_0) - (-1)^i \left[\frac{1}{4}(\Delta - \hbar\omega_0)^2 + \gamma_0^2 g_0^2 \right]^{1/2}, \\ i &= 1, 2. \end{aligned} \quad (3)$$

The $a_{nm}^{1(2)}$ and $b_{nm\mu}^{1(2)}$ depend on the ratio $\hbar\omega_0/\Delta$. It is seen that $|\tilde{\Gamma}_7^n\rangle$ is the same as the original product state. But the nearly degenerate states $|\Gamma_8, 0\rangle$ and $|\Gamma_7, \mu\rangle$ split into the phononlike doublet $|\tilde{\Gamma}_6\rangle$ and the two quartets $|\tilde{\Gamma}_{81(2)}\rangle$. The energy splitting of the latter is $\Delta_v = E_{81} - E_{82}$ and depends on the strength of g_0 and the oscillator strength $\gamma_0^2 = Q_{78} = 5.3$. We have plotted in Fig. 2 the different energies E_α as functions of Δ for a coupling constant $g_0 = 6.3$ K. It has been chosen such that for $\Delta = \hbar\omega_0$ the energies E_{81} and E_{82} agree with the observed Δ_1 and Δ_2 . This figure shows that exact degeneracy of Δ and $\hbar\omega_0$ is certainly not necessary in order to obtain a splitting of the observed size. For $|\Delta - \hbar\omega_0| \gg \gamma_0 g_0$, E_{81} and E_{82}

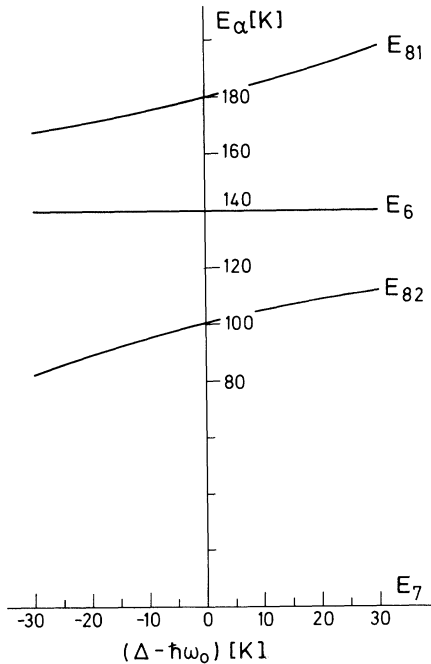


FIG. 2. Vibronic energies as functions of the unperturbed CEF gap Δ with $\hbar\omega_0 = 140$ K and $g_0 = 6.3$ K.

approach $\hbar\omega_0$ and Δ , but these values are reached only slowly.

At this point it is useful to include in the discussion the case of phonon dispersion which has been neglected so far. Then one has to start from Bloch-type CEF states $|\Gamma_\alpha^n(\vec{k})\rangle$ and the vibronic states are superpositions of the form

$$\begin{aligned} |\tilde{\Gamma}_\alpha^n(\vec{q})\rangle &= \sum_{\vec{k}\mu n} u_{\alpha\mu}^{mn}(\vec{k} - \vec{q}) a_{\vec{k} - \vec{q}, \mu}^\dagger |\Gamma_7^n(\vec{k})\rangle \\ &+ \sum_n v_\alpha^{mn}(\vec{q}) |\Gamma_8^n(\vec{q})\rangle. \end{aligned} \quad (4)$$

The eigenvalue equations are then integral equations for those amplitudes. In the "strong-coupling" case, when $g_0\gamma_0/\hbar\omega_b > 1$, where $\omega_b \ll \omega_0$ is a measure of the phonon bandwidth, its solutions correspond to a continuum of phononlike excitations centered around $\hbar\omega_0$ and a bound and anti-bound state. The latter are pushed below and above the phonon continuum. They correspond to the $\tilde{\Gamma}_{82}$ and $\tilde{\Gamma}_{81}$ quartets in the dispersionless model. In the present case $\hbar\omega_b \simeq 20$ K and $g_0\gamma_0/\hbar\omega_b \simeq 2$. We are therefore in the strong-coupling case and neglecting the phonon dispersion is justified.

It is worth pointing out the resemblance of the present problem to that of the exciton-phonon bound states in semiconductors.⁸ Here the CEF excitation and phonons are bound together and propagate through the crystal.

In order to substantiate the above model we compare g_0 as chosen above with the coupling constant g_3 which is determined from a measurement of the c_{44} elastic constant.³ Since g_3 describes the coupling to long-wavelength acoustic phonons, g_0 and g_3 need not be closely related. But a comparison between $g_3^2/c_{44}v_c = 364$ mK (v_c is the volume of the unit cell) and the equivalent $g_0^2/\hbar\omega_0 = 283$ mK shows differences only of the order of 30%. At this stage we mention that explaining the observed two-peak structure by a DJTE would not only require an unrealistic $\hbar\omega_0 = 14$ K but also $g_0^2/\hbar\omega_0 = 64$ K, a value which is by far too large.

Further support for our model is obtained by calculating the dipolar spectral function

$$S(\omega) = \sum_{\substack{\alpha\beta \\ nm}} p_\alpha d_{\alpha\beta} \delta(E_\alpha - E_\beta - \hbar\omega), \quad (5)$$

which determines the magnetic neutron-scattering cross section. Here p_α are the thermal occupation numbers of the vibronic multiplets and $d_{\alpha\beta} = \sum_{mn} |\langle \tilde{\Gamma}_\alpha^n | J_z | \tilde{\Gamma}_\beta^m \rangle|^2$ describes the magnetic dipolar transitions. It is found that there are no

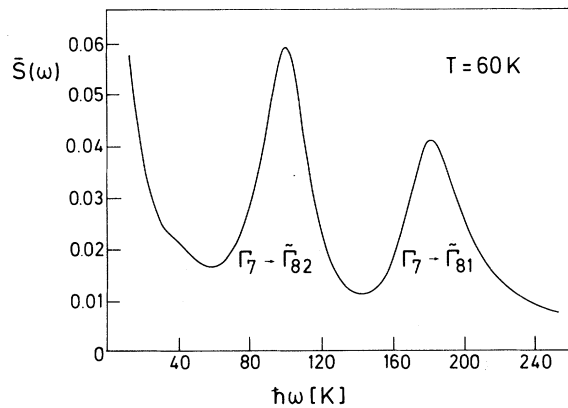


FIG. 3. $\bar{S}(\omega)$ for the vibronic states of CeAl_2 as a result of exchange interaction with conduction electrons where $I_{\text{ex}}N(0) = 0.06$ [I_{ex} is the exchange constant, $N(0)$ is the density of states at the Fermi level].

inelastic *magnetic* transitions between $\tilde{\Gamma}_7$ and $\tilde{\Gamma}_6$, since $\tilde{\Gamma}_6$ is of phonon type. But from what has been said before it is clear that $\tilde{\Gamma}_7$ - $\tilde{\Gamma}_6$ transitions are responsible for the measured peak in the phonon density of states. For $\hbar\omega_0 = \Delta$ the $d_{\alpha\beta}$ are the same when $\tilde{\Gamma}_{81}$ is replaced by $\tilde{\Gamma}_{82}$ and vice versa. This implies two inelastic δ peaks of equal strength as $T \rightarrow 0$. The ratio of the total inelastic to the total elastic scattering rate is found to be 3.2 in agreement with the experiments. In order to account for the observed broadening of the two inelastic peaks we have calculated the relaxation of the vibronic states due to the exchange interaction with the conduction electrons of spin \tilde{s} , $H_{\text{ex}} = -I_{\text{ex}}(g-1)\tilde{s} \cdot \tilde{J}$. The damping mechanism has been studied before for CEF excitations.⁹ When interatomic exchange interactions are neglected the symmetrized spectral function $\bar{S}(\omega) = S(\omega) + S(-\omega)$ can be expressed in terms of the single-ion susceptibility as $\bar{S}(\omega) = \coth(\beta\omega/2)\text{Im}\chi(\omega)$. The latter is calculated with the Mori-Zwanzig technique⁹ to order I_{ex}^2 . We have plotted $\bar{S}(\omega)$ in Fig. 3 with parameters as

indicated there. The frequency integral is normalized to $2\pi\langle J_z^2 \rangle$. It is seen that the exchange interaction shifts some of the intensity to lower frequencies since for $I_{\text{ex}} = 0$ both peaks have equal strength. All this is in qualitative agreement with the experiments. Inclusion of the dispersion for the phonons as well as the CEF excitations would broaden further the inelastic peaks.

Lately it has been found⁵ that selected branches in CeAl_2 show strong low-temperature anomalies which are clearly of magnetoelastic origin as they are absent in LaAl_2 . We expect to be able to explain them within the context of our model by including the $|\Gamma_8, \mu\rangle$ and $|\Gamma_7, \mu, \mu'\rangle$ one- and two-phonon states in the calculations of the phonon spectral function.

In conclusion, we have provided evidence that the anomalies in the inelastic neutron scattering of CeAl_2 are due to a bound state between a CEF excitation and a phonon.

We would like to thank Dr. W. Reichardt and Dr. N. Nücker for making available some of their experimental results before publication.

¹B. Cornut and B. Coqblin, Phys. Rev. B **5**, 4551 (1972).

²F. Steglich, C. D. Bredl, M. Loewenhaupt, and K. D. Schotte, J. Phys. (Paris), Colloq. **40**, C5-301 (1979).

³B. Lüthi and C. Lingner, Z. Phys. B **34**, 157 (1979).

⁴M. Loewenhaupt, B. D. Rainford, and F. Steglich, Phys. Rev. Lett. **42**, 1709 (1979).

⁵W. Reichardt, to be published.

⁶K. R. Lea, M. J. M. Leask, and W. P. Wolf, J. Phys. Chem. Solids **23**, 138 (1962).

⁷J. R. Cullen and A. E. Clark, Phys. Rev. B **15**, 4510 (1977).

⁸Y. Toyozawa and J. Hermanson, Phys. Rev. Lett. **21**, 1637 (1968).

⁹K. W. Becker, P. Fulde, and J. Keller, Z. Phys. B **28**, 9 (1977).